



# A Gq Biased Small Molecule Active at the TSH Receptor

Rauf Latif<sup>1,2\*</sup>, Syed A. Morshed<sup>1,2</sup>, Risheng Ma<sup>1,2</sup>, Bengu Tokat<sup>1†</sup>, Mihaly Mezei<sup>3†</sup> and Terry F. Davies<sup>1,2</sup>

<sup>1</sup> Thyroid Research Unit, Icahn School of Medicine at Mount Sinai, New York, NY, United States, <sup>2</sup> James J. Peters VA Medical Center, New York, NY, United States, <sup>3</sup> Department of Structural and Chemical Biology, Icahn School of Medicine at Mount Sinai, New York, NY, United States

## OPEN ACCESS

### Edited by:

László Hunyady,  
Semmelweis University, Hungary

### Reviewed by:

Stanko S. Stojilkovic,  
National Institutes of Health (NIH),  
United States  
Thierry Durroux,  
Centre National de la Recherche  
Scientifique (CNRS), France

### \*Correspondence:

Rauf Latif  
rauf.latif@mssm.edu

### Specialty section:

This article was submitted to  
Cellular Endocrinology,  
a section of the journal  
Frontiers in Endocrinology

Received: 15 January 2020

Accepted: 11 May 2020

Published: xx May 2020

### Citation:

Latif R, Morshed SA, Ma R, Tokat B, Mezei M and Davies TF (2020) A Gq Biased Small Molecule Active at the TSH Receptor. *Front. Endocrinol.* 11:372.  
doi: 10.3389/fendo.2020.00372

G protein coupled receptors (GPCRs) can lead to G protein and non-G protein initiated signals. By virtue of its structural property, the TSH receptor (TSHR) has a unique ability to engage different G proteins making it highly amenable to selective signaling. In this study, we describe the identification and characterization of a novel small molecule agonist to the TSHR which induces primary engagement with G<sub>q/11</sub>. To identify allosteric modulators inducing selective signaling of the TSHR we used a transcriptional-based luciferase assay system with CHO-TSHR cells stably expressing response elements (CRE, NFAT, SRF, or SRE) that were capable of measuring signals emanating from the coupling of G<sub>αS</sub>, G<sub>αq/11</sub>, G<sub>βγ</sub>, and G<sub>α12/13</sub>, respectively. Using this system, TSH activated G<sub>αS</sub>, G<sub>αq/11</sub>, and G<sub>α12/13</sub> but not G<sub>βγ</sub>. On screening a library of 50K molecules at 0.1, 1.0 and 10 μM, we identified a novel G<sub>q/11</sub> agonist (named MSq1) which activated G<sub>q/11</sub> mediated NFAT-luciferase <4 fold above baseline and had an EC<sub>50</sub> = 8.3 × 10<sup>-9</sup> M with only minor induction of G<sub>αS</sub> and cAMP. Furthermore, MSq1 is chemically and structurally distinct from any of our previously reported TSHR agonist molecules. Docking studies using a TSHR transmembrane domain (TMD) model indicated that MSq1 had contact points on helices H1, H2, H3, and H7 in the hydrophobic pocket of the TMD and also with the extracellular loops. On co-treatment with TSH, MSq1 suppressed TSH-induced proliferation of thyrocytes in a dose-dependent manner but lacked the intrinsic ability to influence basal thyrocyte proliferation. This unexpected inhibitory property of MSq1 could be blocked in the presence of a PKC inhibitor resulting in derepressing TSH induced protein kinase A (PKA) signals and resulting in the induction of proliferation. Thus, the inhibitory effect of MSq1 on proliferation resided in its capacity to overtly activate protein kinase C (PKC) which in turn suppressed the proliferative signal induced by activation of the predominant cAMP-PKA pathway of the TSHR. Treatment of rat thyroid cells (FRTL5) with MSq1 did not show any upregulation of gene expression of the key thyroid specific markers such as thyroglobulin(Tg), thyroid peroxidase (Tpo), sodium iodide symporter (Nis), and the TSH receptor (Tshr) further suggesting lack of involvement of MSq1 and

$G\alpha_q/11$  activation with cellular differentiation. In summary, we identified and characterized a novel  $G\alpha_q/11$  agonist molecule acting at the TSHR and which showed a marked anti-proliferative ability. Hence, Gq biased activation of the TSHR is capable of ameliorating the proliferative signals from its orthosteric ligand and may offer a therapeutic option for thyroid growth modulation.

**Keywords:** TSH, GPCR, gprotein, proliferation, agonist

## INTRODUCTION

Traditionally GPCR drug development has focused on conventional agonists and antagonists that are known to act as “on-off” switches. However, there is growing appreciation that GPCRs can mediate their physiologically relevant effects through selective signaling due to subtle structural changes and engagement of G protein and non-G protein effectors. Selective signaling can be driven by endogenous ligands, synthetic peptides or small molecules, which bind to the orthosteric or allosteric site(s) and in turn bias the downstream signal. The TSHR which is made up of a large glycosylated ectodomain and seven transmembrane helices which are connected by extracellular and intracellular loops (1) is structurally poised as a candidate for allosteric modulation with its ability to engage all four classes of G proteins (2). Studies using both modeling and mutational analysis of the TSHR have indicated the structural determinants of the G protein coupling to the receptor (3, 4). However, it is not yet fully clear as to what preferential order these different G proteins are engaged by the TSHR during activation nor the exact intra- and -inter molecular interactions leading to coupling of the different G proteins by TSH or TSHR antibodies. However, crystallization of the partial ectodomain with stimulating and blocking autoantibodies (5-7) together with studies of the molecular rearrangement of the TSHR ectodomain and hinge regions has given some recent insight into the possible mechanism(s) of this activation (8, 9).

Small molecules can bind to the allosteric sites on the TSHR TMD and ectodomain (10, 11) and are excellent tools to gain insight into the potential for TSHR selective signaling. Their unique ability to readily permeate the cell membrane and interact with specific residues within the transmembrane helices can induce subtle conformational changes (12–14). In recent years there has been rapid development of small molecules, both agonists (15–17) and antagonists (16, 18–20) against the TSHR as part of a search for novel therapeutic agents. These various small molecule ligands induce the  $G\alpha_s$  pathway of the TSHR and the possibility of selective  $G\alpha_{q/11}$  activation by a small molecule has not been explored. However, studies have indicated that such selectivity in signaling can be established in GPCRs and not only by different receptor subtypes (21, 22) but also via pathway bias suggesting ligand selectivity can be a potential source of a defined pharmacology for small molecules (23, 24).

In this report, we describe the identification and *in vitro* characterization of a novel small molecule that activates the TSHR by preferentially initiating  $G\alpha_{q/11}$  signaling and then examined its biological consequences on thyrocyte proliferation and gene expression.

## MATERIALS AND METHODS

## Establishing Double Transfected CHO-TSHR Cell Lines

In order to identify the signaling through the four major classes of G-proteins ( $G_{\alpha s}$ ,  $G_{\alpha q/11}$  and  $G_{\alpha 12/13}$  and  $G_{\beta\gamma/i}$ ) by the TSHR, we generated double transfected CHO-TSHR stable lines containing CRE, NFAT, SRF, or SRE response elements (RE) tagged to a modified form of luciferase reporter. These double transfected stable clones were established by selecting the cells with hygromycin (800  $\mu$ g/ml) and 500  $\mu$ g/ml of G418 (neomycin sulfate). Following initial screening and validation, these stable cell lines were maintained in Ham's F-12 medium with 10% fetal bovine serum (FBS), 100 units of penicillin and streptomycin with 200  $\mu$ g/ml of hygromycin and G418 to maintain the selection pressure in these co-transfected cells. Using the individually co-transfected stable lines containing the respective response elements, we screened a 50K chemical library at 0.1, 1 and 10  $\mu$ M against CRE, NFAT, SRF, and SRE cells in a 384 well format following the protocol described previously (17).

## Treatment and Lysate Preparation

For downstream signaling studies, low passage number of FRTL5 cells were cultured in 60 mm dishes using Hams F12 medium with 5% calf serum to which 1X 6H (6 hormone mixture) was added as previously described (25). Once the cells reached 60–80% confluence, cells were washed twice with plain medium and then cultured further in Ham F12 medium containing only 5H hormone (-TSH) for 72 hrs. Following this the cells were washed twice with plain F12 medium and incubated for another 48 h in Ham's F12 medium containing 0.3% BSA (basal medium). These cells were then either stimulated with increasing doses of MSq1, TSH or MS438 or combination of TSH plus MSq1 or TSH+MSq1+ PKC inhibitor at 2  $\mu$ M (G06883) as per the experimental details described under figure legends for 48 h at 37C. Lysates from these treated cells were prepared using 1X Novagen phosphosafe extraction buffer as per the manufacturer's instructions and total protein in the lysate estimated by Bradford (26). Further the proteins were resolved on 4–15% SDS-PAGE and transferred to PVDF membranes by wet transfer and classic immunoblotting performed for detection of phospho protein after

**Abbreviations:** TSHR, Thyroid stimulating receptor; GPCR, G protein coupled receptors; GD, Graves' disease; TMD, transmembrane domain; GAPDH, glyceraldehyde-3-phosphate dehydrogenase.

229 blocking membranes with 2% BSA for 2 h at RT or subjected  
 230 to protein quantification using simple western system by the  
 231 WES machine for immunoblotting and detection (ProteinSimple,  
 232 Santa Clara, CA, USA).

### 233 Immunoblotting and Detection

234 In the present study, we quantitated the absolute response to  
 235 PKC and PKA in the lysate prepared from the treated cells as  
 236 described above. pPKC was detected by classical immunoblotting  
 237 procedure described earlier (27) using commercially obtained  
 238 primary antibodies to pPKC  $\beta$ II ser660, Anti-rabbit HRP  
 239 (1:20,000) in 1X tris-borate saline with tween 20 0.5% (TBST)  
 240 was used as detection antibody and the immunoblots developed  
 241 with ECL. Quantitation of pPKA was carried out using the  
 242 protein simple WES system after titrating the primary and  
 243 secondary antibodies against different concentrations of the  
 244 samples. Briefly, the WES protocol is as described here, first,  
 245 a 0.2  $\mu$ g of lysate was mixed with master mix to achieve a final  
 246 concentration of 1X sample buffer in the presence of fluorescent  
 247 molecular weight marker and 40 mM dithiothreitol, the samples  
 248 were denatured at 95°C for 5 min. Target proteins were immuno-  
 249 probed with primary antibody pPKA (thr197) followed by HRP-  
 250 conjugated secondary antibodies. All antibodies were diluted  
 251 using an antibody diluent at a 1:100 or 1:200. Detection of  
 252 ERK 44-kDa protein in the lysate using anti ERK served as  
 253 a positive run control in addition to the biotinylated ladder  
 254 for size estimation.  $\beta$ -actin was used as the loading control.  
 255 Digital images of the signal were analyzed with Compass software  
 256 (ProteinSimple), and the quantified data of the detected proteins  
 257 with the correct molecular weight is reported as signal/noise ratio  
 258 derived from average signal intensity exposures.

### 260 Proliferation Measured by Alamar Blue

261 Proliferation of FRTL5 cells was measured using Alamar Blue,  
 262 which monitors the reducing environment of the living cell.  
 263 The active ingredient is resazurin, which is a stable, nontoxic  
 264 and permeable compound, which accepts electrons and changes  
 265 from the oxidized, non-fluorescent, blue state to the reduced,  
 266 fluorescent, pink state. These studies were carried out on FRTL5  
 267 grown on black clear bottom 96 well plates. Cells in the log phase  
 268 were harvested by trypsin and seeded as  $30 \times 10^3$  cells/well and  
 269 allowed to adhere to the bottom of plate in complete HamF12  
 270 medium by incubating the cells with 6H overnight at 37°C.  
 271 Following a 24 to 36 hrs incubation, the cells were culturally  
 272 prepared by removing TSH for 3 days prior to induction of  
 273 proliferation as described earlier. The cells were then exposed  
 274 to MSq1, TSH or combination of both with and without the  
 275 PKC inhibitor as per the experiment described under figure  
 276 legends. For determining the effect of a small molecule or  
 277 TSH on cell growth, we had stimulated vs. unstimulated cells.  
 278 Following 48 h of treatment, Alamar Blue was aseptically added  
 279 to each well in an amount equal to 10% of the volume in the  
 280 wells. Cells with Alamar Blue were further incubated at 37°C  
 281 for another 5 h prior to reading the plates. Proliferation was  
 282 assessed by measuring fluorescence intensity of the reduced dye  
 283 at 540/580 nm. Wells with media plus dye only was used as the  
 284 background control. Log change between untreated over that

285 of treated groups was deduced from the fluorescent intensities  
 286 obtained after background subtraction.

### 287 Docking and Contact sites

288 Docking of the lead MSq1 molecules was performed on a  
 289 homology model of the TSHR-TMD based on rhodopsin  
 290 (PDB:1F88). This template was chosen because of the low RMSD  
 291 values between the backbone of the TM helices of the TSHR  
 292 model and that of the rhodopsin x-ray crystal structure (14)  
 293 and fits the experimental parameters that we have previously  
 294 described (15). The initial homology model of rhodopsin TMD  
 295 was obtained from the Uniprot server (<http://www.uniprot.org>).  
 296 The conformations of the extracellular loops were constructed  
 297 with a Monte Carlo method (16). The 3D geometries of the  
 298 docked ligands were generated with MarvinSketch (<http://www.chemaxon.com>). Multiple docking was carried out using the  
 299 programs Glide, Autodock-4 and Autodock-Vina. The docking  
 300 results were analyzed using Dockres and other supporting script  
 301 tools (17). In particular, Dockres extracts the coordinates of the  
 302 docked poses from the docking log file and identifies contacts  
 303 between the ligand and target as pairs of mutually proximal atoms  
 304 and hydrogen bonds (if any) as X...H-X' where X and X' are  
 305 polar atoms (one on the ligand and the other on the target) with  
 306 X...H distance within threshold and X...H-X angle is greater  
 307 than 120 deg.

### 313 IP-One Assay

314 In principle PLC is the main intracellular effector enzyme of  
 315  $G\alpha_{q/11}$ -coupled GPCRs. PLC hydrolyzes PIP<sub>2</sub> into IP<sub>3</sub> and DAG.  
 316 The intracellular second messenger IP<sub>3</sub> is rapidly degraded by  
 317 phosphatases and recycled back via inositol into cell membrane  
 318 PIP<sub>2</sub>. Thus, for measuring  $G\alpha_{q/11}$  activation by MSq1 in  
 319 CHOTSHR cells we used the Cisbio IP-One Gq kit which is  
 320 a competitive immunoassay intended to measure myo-inositol-  
 321 1phosphate (IP1) accumulation in cells. The inositol phosphate  
 322 accumulation assay utilizes the ability of lithium to inhibit  
 323 the breakdown of inositol monophosphates and detects this  
 324 accumulated IP1 by HTRF® technology. In the assay native IP1  
 325 produced by cells or unlabeled IP1 (standard curve) compete  
 326 with d2-labeled IP1 (acceptor) for binding to anti-IP1-Cryptate  
 327 (donor). The specific signal (i.e., energy transfer) is inversely  
 328 proportional to the concentration of IP1 in the standard or  
 329 sample.  $50 \times 10^3$  CHOTSHR cells per well were seeded in 96  
 330 well black plates in complete Hams F12 medium and incubated  
 331 overnight at 37°C. The adherent cells were gently washed once  
 332 with warm plain medium with low serum (2%) and the cells  
 333 were treated with increasing doses of TSH ( $\mu$ U) or MSq1 ( $\mu$ M)  
 334 in stimulation buffer containing 50 mM of lithium chloride. At  
 335 the end of 2 h incubation the cells were lysed using the lysis  
 336 buffer provided and treated with detection antibodies as per  
 337 manufacturer's instructions and run along with the standards  
 338 provided in the kit. The measurement of acceptor (665 nm) to  
 339 donor (620 nM) emission was obtained using the microplate  
 340 plate reader ClarioStar and ratio calculated and interpolated to  
 341 standard curves to calculate the values of the unknown samples.

## 343 TSHR Expression by Flow-Cytometry

344 ML-1 and FT236, two follicular cancer lines, were grown in  
 345 DMEM high glucose with 10 % FBS, 200 mM glutamine, 1x  
 346 sodium pyruvate 1X Minimum essential medium with 100 units  
 347 of penicillin and streptomycin. The cells were detached from the  
 348 plate non-enzymatically using 1 mM EGTA/EDTA and washed  
 349 twice with 1X PBS, filtered using 75  $\mu$ M filter and total cells  
 350 counted.  $0.5 \times 10^6$  cells/tube were suspended in 100  $\mu$ l of  
 351 FACS staining buffer (1X PBS with 0.2% sodium azide and  
 352 2% FBS) with anti TSHR mAb RSR1 mouse Mab (0.1  $\mu$ g/ml)  
 353 and incubated for 1 h at room temperature. Following 2x wash  
 354 with FACS buffer (1XPBS with 0.02% sodium azide) and the  
 355 bound TSHR receptor antibodies were detected using anti-mouse  
 356 antibody Fab' phycoerthrin (PE) labeled secondary antibody at  
 357 1:200. Unstained cells, isotype antibody or secondary antibody  
 358 alone were used as controls in the assay. The results were  
 359 expressed as the percentage positive cells detected in the test  
 360 samples compared to the controls by the vertical gates assigned  
 361 based on the controls.

## 363 Gene Expression

364 For gene expression analysis, total RNA was extracted  
 365 using a RNeasy kit and was treated with ribonuclease-free  
 366 deoxyribonuclease. Five micrograms of total RNA were reverse  
 367 transcribed into cDNA using the SuperScript III system. All  
 368 Q-PCRs was performed using the Step OnePlus Real-time  
 369 PCR system (Applied Biosystems, Foster City, CA). The  
 370 reactions were established with 10  $\mu$ L of SYBR Green master  
 371 mix (Applied Biosystems, Foster City, CA), 0.4  $\mu$ l (2  $\mu$ M)  
 372 of sense/anti-sense gene-specific primers, 2  $\mu$ l of cDNA and  
 373 DEPC-treated water to a final volume of 20  $\mu$ l. The PCR  
 374 reaction mix was denatured at 95°C for 60 s before the first  
 375 PCR cycle. The thermal cycle profile was used is as follows:  
 376 denaturizing for 30 s at 95°C; annealing for 30 s at 57–60°C  
 377 (dependent on primers); and extension for 60 s at 72°C. A total  
 378 of 40 PCR cycles were used. For each target gene, the relative  
 379 gene expression was normalized to that of the glyceraldehyde-3-  
 380 phosphate dehydrogenase (GAPDH) housekeeping gene. Data  
 381 presented as fold change in relative gene expression are from two  
 382 independent experiments in which all sample sets was analyzed  
 383 in triplicate.

## 386 Statistical Analyses

387 All curve fitting and P value calculations (one-way ANOVA)  
 388 were carried using GraphPad Prism 5 software. All assays  
 389 were performed at least 2 or 3 times as indicated. In case of  
 390 immunoblot one representative experiment is shown.

## 393 RESULTS

### 395 Identification of a Unique Gq Activator

396 In order to identify allosteric ligands that can activate different  
 397 G proteins of the TSHR we first developed a series of CHO-  
 398 TSHR cells that were transfected with different response elements  
 399 tagged to luciferase that can specifically identify the activation

400 of specific G proteins as indicated schematically in **Figure 1A**.  
 401 The activation of these different response elements was validated  
 402 using bovine TSH as indicated in **Figure 1B**. This analysis clearly  
 403 indicated that TSH was capable of activating  $\text{G}\alpha_s$ ,  $\text{G}\alpha_{q/11}$ , and  
 404  $\text{G}\alpha_{12/13}$  in a dose-dependent manner. No activation was observed  
 405 of  $\text{G}\beta\gamma$  in this system. The respective positive controls used for  
 406 each of the response elements are indicated and explained in the  
 407 figure legends.

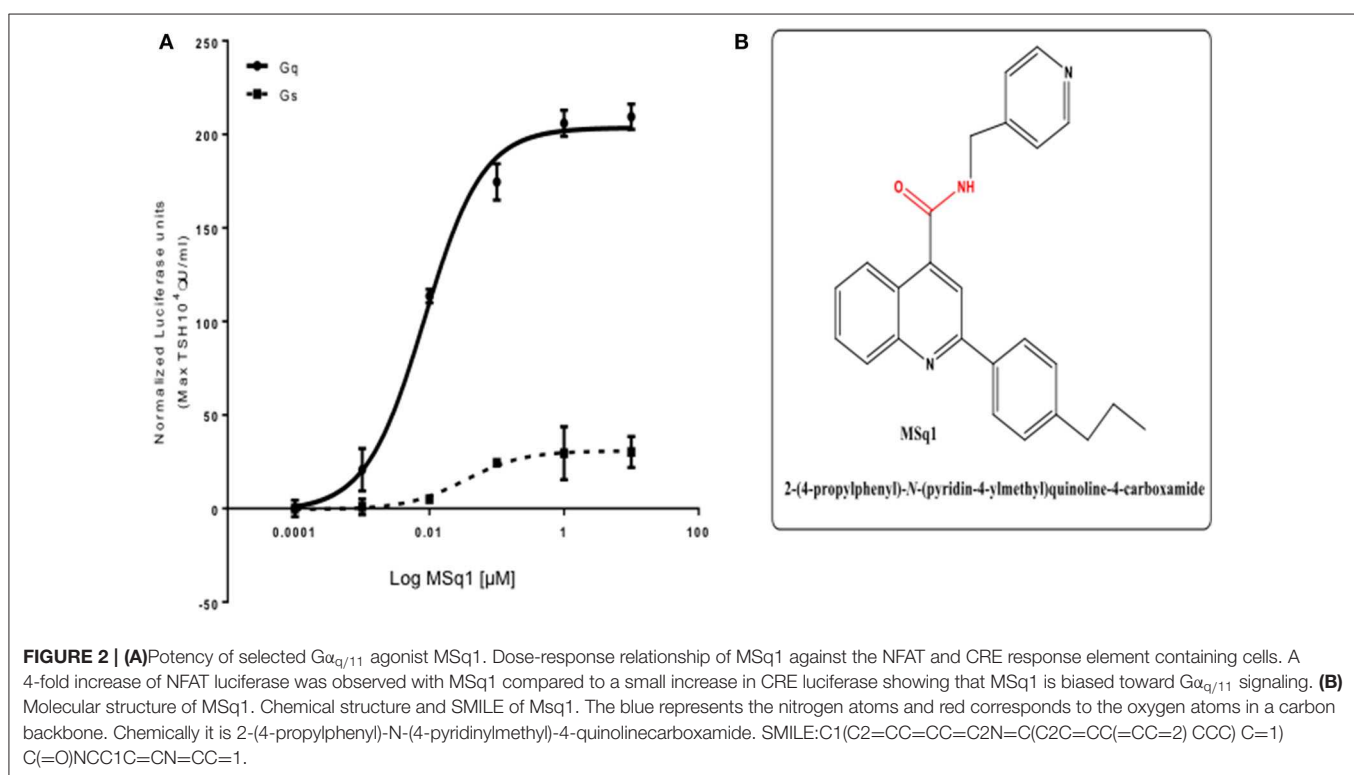
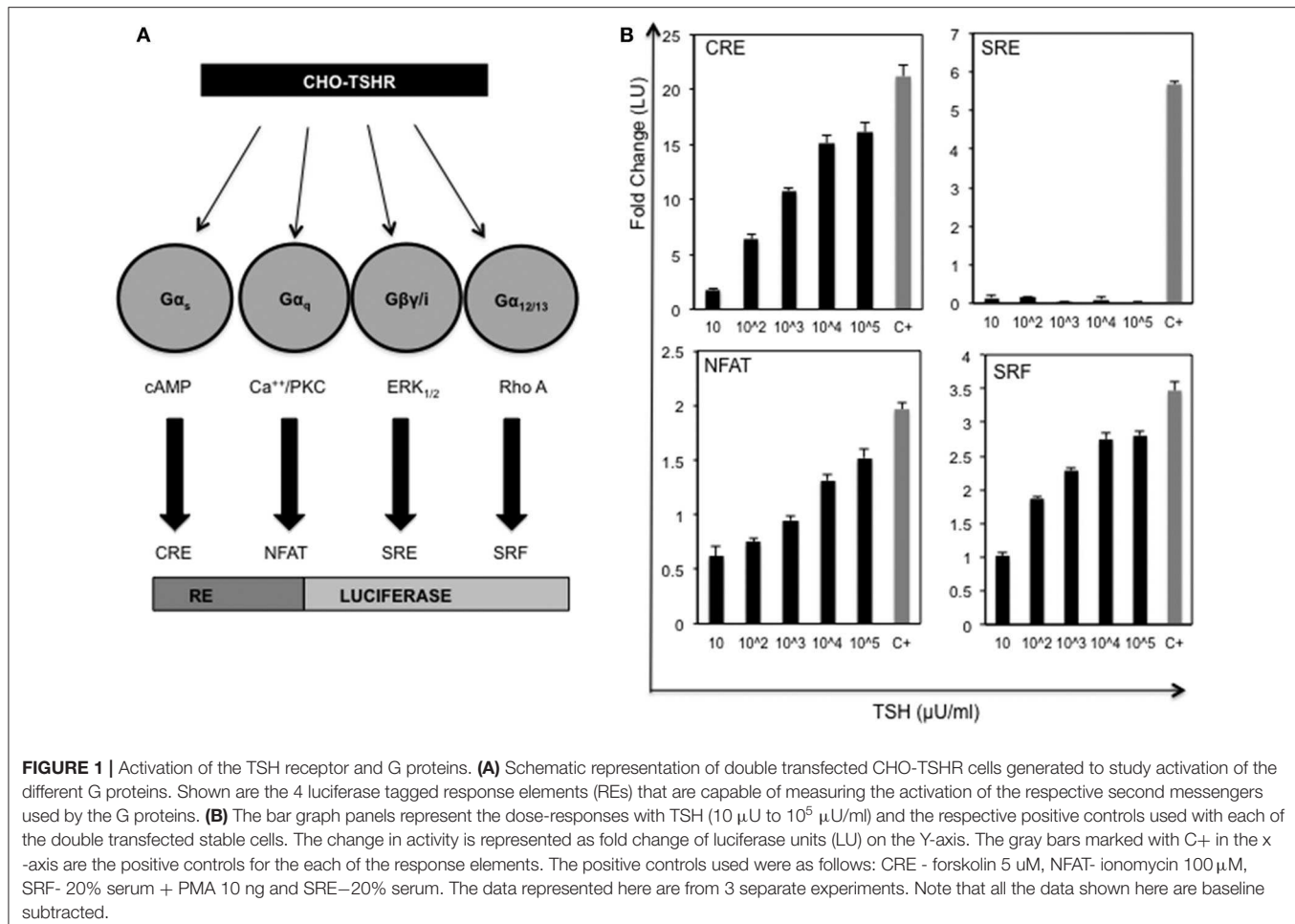
408 Screening a 50K library at 0.1,1 and 10  $\mu$ M against  
 409 this panel of stable CHO TSHR luciferase cells allowed us  
 410 to identify a small molecule, which preferentially activated  
 411 CHO-TSHR-NFAT luciferase cells. Further examination of  
 412 this Gq activator (named MSq1) against CHOTSHR-NFAT,  
 413 which couples  $\text{G}\alpha_{q/11}$ , and CHOTSHR-CRE, which measures  
 414 activation via  $\text{G}\alpha_s$ , in a dose-dependent manner (**Figure 2A**)  
 415 showed MSq1 to be a potent activator of Gq with an  $\text{EC}_{50} = 8.3 \times 10^{-9}\text{M}$  after normalizing the data to max TSH  
 416 ( $10^4\mu\text{M}/\text{ml}$ ). MSq1 had only minor activation toward  $\text{G}\alpha_s$  thus  
 417 making this molecule a preferential Gq activator. Structurally  
 418 this molecule differed from any of the known agonist or  
 419 antagonist small molecules (**Figure 2B**). Control studies with  
 420 MSq1 measuring its influence on activation in normal CHO  
 421 cells (without a TSHR) but transfected with either NFAT  
 422 luciferase or CRE luciferase at 10  $\mu\text{M}$  showed no activation of  
 423 luciferase (**Figure S1**). We have shown that MSq1 is incapable  
 424 of activating either  $\text{G}\beta\gamma$  or  $\text{G}_{12/13}$  using the luciferase system  
 425 further confirming that this is a  $\text{G}_{q/11}$  biased novel small molecule  
 426 (**Figure S2**).

### 428 Binding Sites of MSq1 by Docking Studies

429 We examined the binding sites of this Gq activator by *in-*  
 430 *silico* docking using the structure of the TSHR TMD region  
 431 developed by homology modeling and based on the rhodopsin  
 432 crystal structure (as detailed in Methods). Using the top  
 433 scoring docking poses generated by Autodock-4 and the  
 434 criteria of  $\leq 4\text{\AA}$ , the putative contact points of MSq1 within  
 435 the TSHR TMD were deduced. Like most allosteric small  
 436 molecules against the TSHR, the MSq1 sites were nestled in  
 437 the “hydrophobic pocket” formed by the different helices within  
 438 the TSHR TMD (**Figure 3A**). Further analysis indicated that  
 439 MSq1 made major contact points on the TSHR TMD helices  
 440 H1, H2, H3, and H7 within the hydrophobic pocket and the  
 441 extracellular loops including L2-3 & L4-5 (**Figure 3B**). When  
 442 these contact residues were compared to our  $\text{G}\alpha_s$  agonist  
 443 MS438 some overlapping, and some unique residues could  
 444 be observed as shown in **Table 1** which lists the top-scoring  
 445 Glide, Autodock-4 and Autodock-Vina poses for both MS438  
 446 and MSq1.

### 449 Downstream Signaling of the Gq Activator

450 Since the *in-silico* modeling confirmed the potential binding of  
 451 MSq1 to the TSHR TMD, we examined the key downstream  
 452 signals that are known \*\*\* to be driven by Gq activation.  
 453 Activation of PLC was assayed by measuring IP1 accumulation,  
 454 which showed that MSq1 and TSH were capable of significantly  
 455 increasing IP1 generation (**Figure 4A** inset). Furthermore,



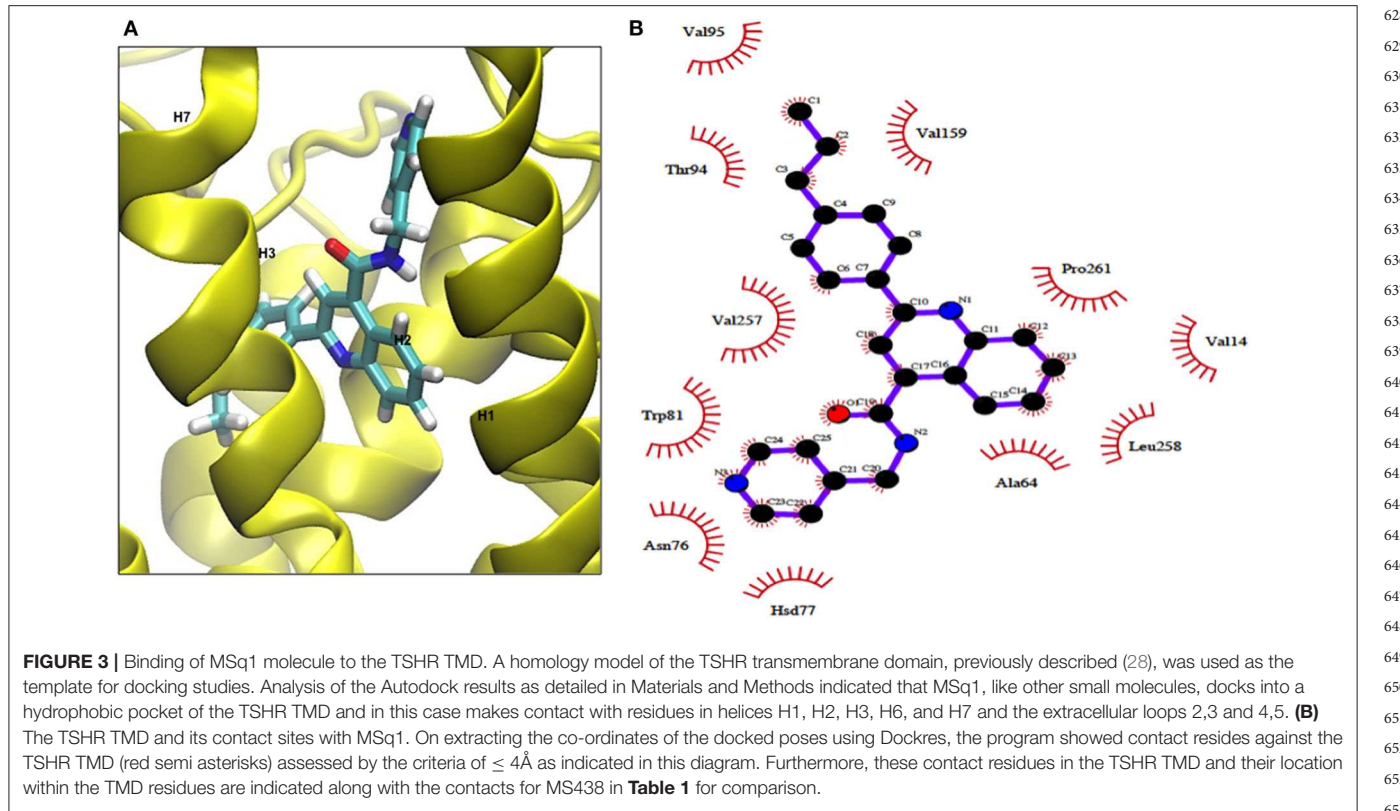


**TABLE 1 |** TSHR residues on the TMD that MSq1 and MS438 contact.

| TSHR residue | Residue No # | Ballest # | MS438   |         |         | MSq1    |         |         |
|--------------|--------------|-----------|---------|---------|---------|---------|---------|---------|
|              |              |           | rG(I-P) | rA(L-P) | rV(I-P) | rG(L-P) | rA(L-P) | rV(L-P) |
| LEU          | 10           | 1.35      |         | 3.1     | 3.6     |         | 3.1     |         |
| VAL          | 14           | 1.39      |         |         | 3.2     |         |         | 3.4     |
| VAL          | 17           | 1.42      |         |         | 3.4     |         |         |         |
| LEU          | 60           | 2.57      |         | 3.2     | 3.2     |         |         | 3.2     |
| LEU          | 61           | 2.58      |         | 3.2     | 3.1     |         |         |         |
| ALA          | 64           | 2.57      | 2.9     | 2.8     | 3.5     | 2.9     | 2.8     |         |
| ASN          | 76           | L (2-3)   | 3.1     | 2.8     | 3.6     | 2.9     |         |         |
| TRP          | 81           | L (2-3)   |         |         | 3.8     | 3.1     |         |         |
| CYS          | 87           | 3.25      | 3.6     |         |         | 3.6     |         |         |
| ALA          | 90           | 3.28      | 4.0     |         | 3.7     | 4.0     |         |         |
| GLY          | 91           | 3.29      | 3.0     |         | 3.6     |         |         | 3.6     |
| THR          | 94           | 3.32      |         | 2.8     | 2.7     | 3.8     | 3.5     | 3.7     |
| VAL          | 95           | 3.33      |         | 3.1     | 3.6     |         | 3.1     | 3.6     |
| SER          | 98           | 3.36      |         | 3.3     | 3.4     |         | 3.4     | 3.4     |
| GLU          | 99           | 3.37      |         |         | 3.7     |         |         |         |
| LYS          | 158          | L (4-5)   |         | 3.2     |         |         |         |         |
| VAL          | 159          | L (4-5)   |         | 3.4     | 3.5     | 3.7     |         | 4.1     |
| ILE          | 233          | 6.51      |         | 3.2     | 3.4     |         |         | 3.4     |
| LYS          | 253          | 7.42      |         | 3.3     | 3.8     |         | 3.3     |         |
| ILE          | 254          | 7.43      |         | 3.3     |         |         |         |         |
| VAL          | 257          | 7.46      | 3.7     | 2.7     | 3.6     | 3.2     | 3.3     | 3.4     |
| LEU          | 258          | 7.47      |         | 3.1     | 3.2     |         | 3.5     | 3.4     |
| TYR          | 260          | 7.49      |         | 3.2     |         |         | 3.5     |         |
| PRO          | 261          | 7.50      | 3.1     | 3.0     | 3.6     | 3.1     |         | 3.7     |

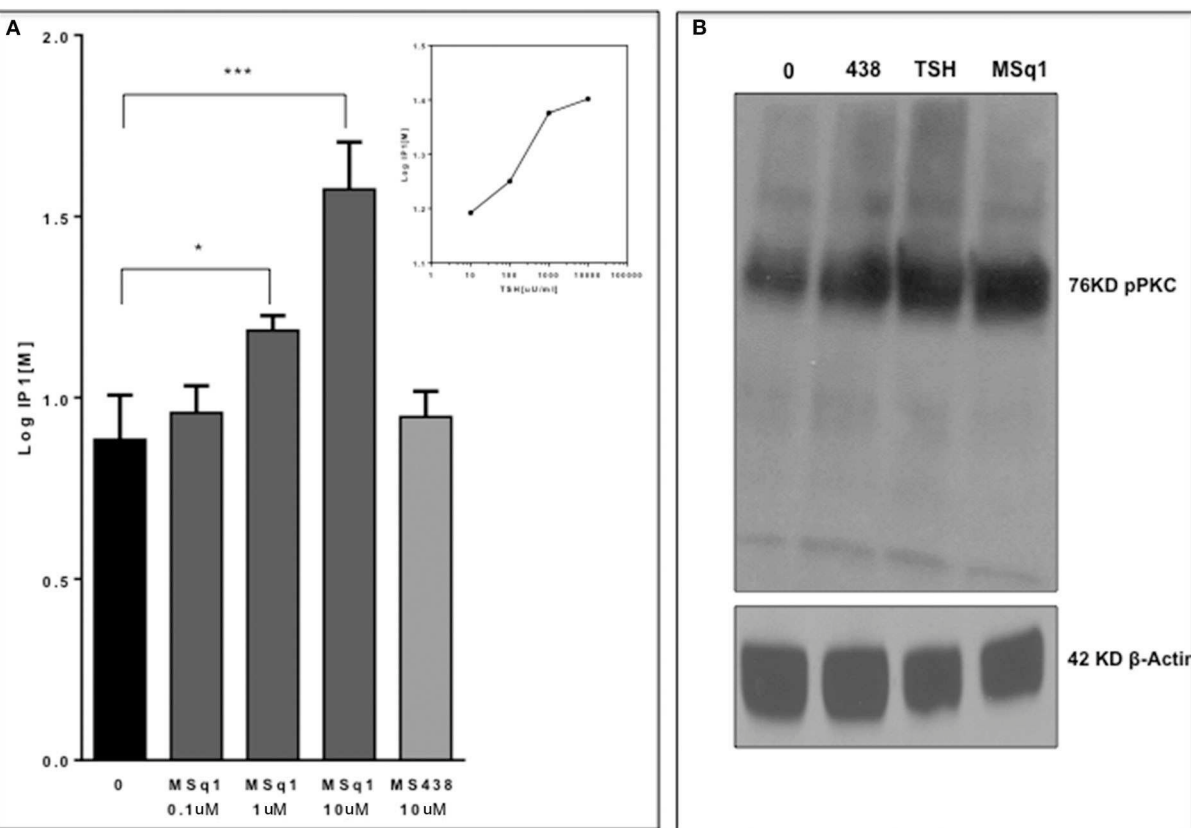


**FIGURE 4 |** Gq signaling by MSq1. **(A)** Since Gq activation is known to result in an IP1 increase via PLC- $\beta$  activation, we measured IP activation in CHO-TSHR cells with MSq1 at 0.1 and 10  $\mu$ M. As indicated here MSq1 showed a significant increase ( $P = 0.03$ ) in IP1 on stimulation with MSq1 which was not observed by MS438 even at 10  $\mu$ M. The inset shows the dose dependent increase in IP1 with TSH. The data is plotted after background subtraction. **(B)** Total lysates of FRTL5 cells treated with MS438 10  $\mu$ M, TSH 1,000  $\mu$ U/ml and MSq1 10  $\mu$ M for 24 h and the immunoblots probed for pPKC. MSq1 increased pPKC when compared to the unstimulated cells (lane 0). The 42KD  $\beta$  actin was used as the loading control. ( $^*P < 0.05$ ), ( $^{***}P < 0.0001$ ).

using phospho-specific antibodies against PKC, we observed that MSq1 significantly enhanced pPKC compared to both TSH and MS438 in thyroid (FRTL5) cells (Figure 4B, upper panel). However, no significant enhancement of pERK or pAKT was observed by MSq1 activation (Figure 4B, lower panel). These downstream signaling studies indicated that MSq1 had the ability to activate the two major arms of  $\text{G}\alpha_{q/11}$  signaling as shown by NFAT-luciferase activation and enhanced PKC activation.

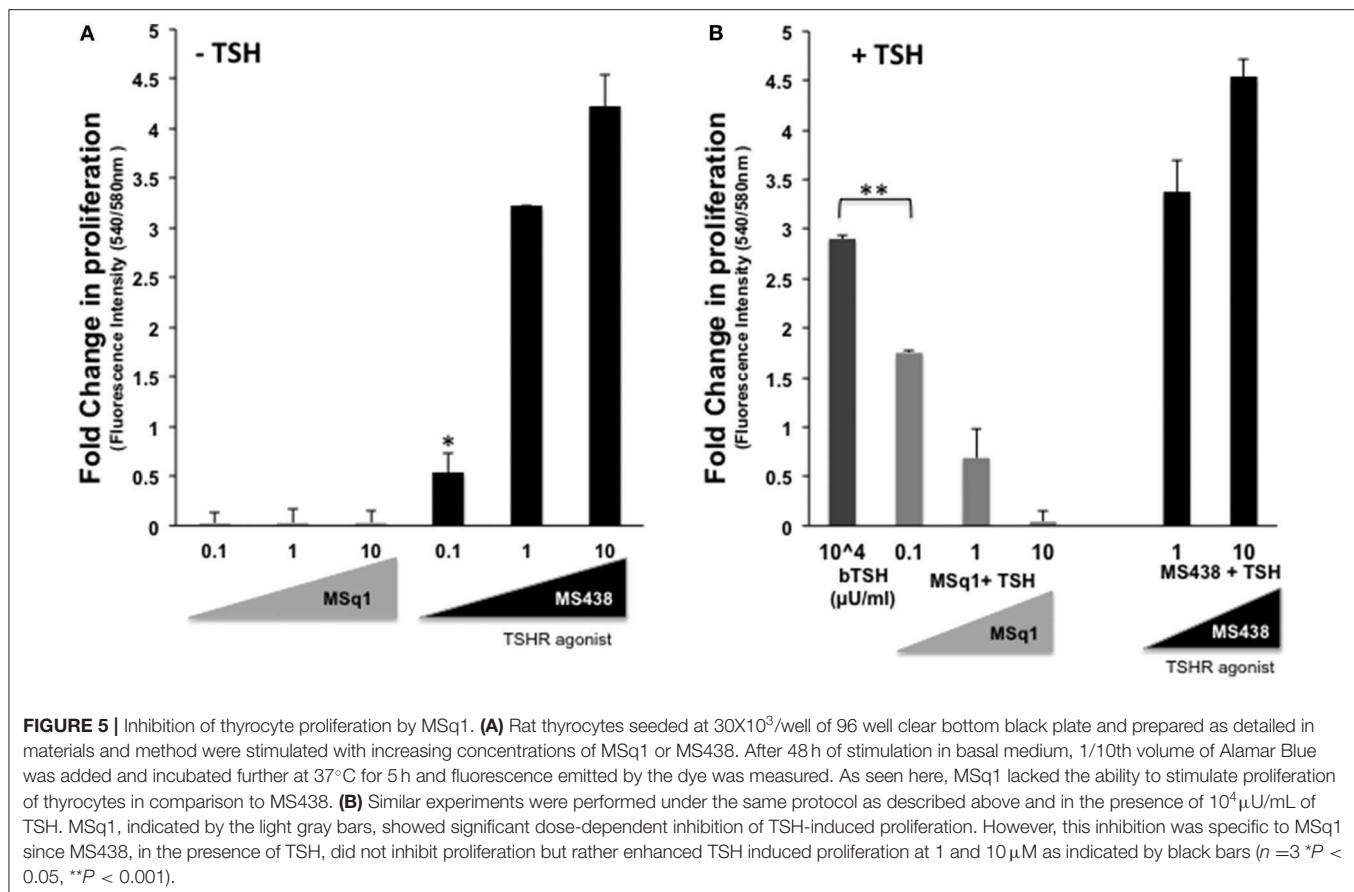
### Inhibition of TSH Induced Proliferation by Gq Activation

The physiological significance of cAMP signaling by  $\text{G}\alpha_{q/11}$  coupling on thyrocyte growth and proliferation is well-established. Since the effect of  $\text{G}\alpha_{q/11}$  on thyroid cell proliferation is not clear we examined the action of MSq1 on proliferation of thyrocytes using rat FRTL5 cells. As indicated in Figure 5A, MSq1 failed to enhance basal proliferation of thyrocytes while one of our previously published TSHR agonists (MS438) showed a dose-dependent increase in proliferation and which is known to activate the cAMP-PKA pathway like TSH. In contrast,

in the presence of  $10^4$   $\mu$ U/ml of TSH, MSq1 inhibited the TSH induced proliferation of thyrocytes in a dose-dependent manner suggesting a suppressive action of Gq activation on the proliferative capacity of the TSH induced Gs-cAMP-PKA pathway (Figure 5B). This inhibition was only observed in TSH dependent thyrocytes and ML-1 cells derived from a human follicular carcinoma line with a high expression of TSHRs (75% expression of cell surface TSHR as established by flow cytometry) (Figure 6A) or FTC 236 cells, another follicular carcinoma line which totally lacks cell surface TSHR (Figure 6B), did not respond to MSq1 actions (Figures 6C,D). Examining gene expression for common thyroid differentiation markers such sodium iodide symporter (NIS), thyroglobulin (Tg) and the TSHR by qPCR, we did not find these markers to be upregulated in treated cells, suggesting that MSq1 activation of  $\text{G}\alpha_{q/11}$  lacked the ability to affect thyrocyte differentiation markers (Figure S3).

### Release of Inhibitory Effect on Proliferation by PKC Inhibition

In order to examine the mechanism of the suppression of TSH induced thyroid cell proliferation we used a broad-spectrum



PKC inhibitor (G06983) in the presence of TSH and MSq1. As shown earlier, MSq1 treatment at  $10 \mu\text{M}$  caused inhibition of TSH induced proliferation. However, in the presence of the PKC inhibitor, inhibition of proliferation by MSq1 was markedly reduced (Figure 7A). On quantitating the PKA signal using Western blotting with an anti PKA antibody, we observed that cells treated with TSH and MSq1 in the presence of the PKC inhibitor for 48 h showed significantly enhanced PKA signals compared to MSq1 plus TSH or TSH alone (Figures 7B,C). These data demonstrated that enhancement of the PKC signal by MSq1 inhibited the cAMP-PKA pathway induced by TSH activation in the thyrocytes.

## DISCUSSION

TSH is known to induce engagement of all four classes of G protein (2) with the TSHR. However, the major pathway activated by TSH is the  $\text{G}\alpha_s$  pathway via PKA (29). The consequence of changing this selection is not well-understood. In particular, the role of the  $\text{G}\alpha_{q/11}$  pathway via PKC has not been clearly clarified and it is unclear whether overt activation of this pathway has any cellular consequences. Therefore, identifying selective allosteric activators, which are biased to activating a G protein class, is one way of studying the mechanism of TSHR selective signaling and its physiological or pathophysiological effects on thyroid

and extra thyroidal TSHRs. This is especially so when knock-out mouse models, which although a very valuable research tool for studying gene function, have their limitations in terms of producing an observable change and may even produce unexpected characteristics which in certain situations cannot be extrapolated to humans (30). In this report, we present data on the identification of a potent  $\text{G}\alpha_{q/11}$  activator against the TSHR and our examination of its effects on thyrocytes.

In recent years high-throughput screening assays, combined with *in silico* structural approaches and medicinal manipulations, have resulted in the identification of a number of specific and potent agonists (16, 17, 31) and antagonists (18, 19, 32) against the TSHR which effectively activate or inhibit  $\text{G}\alpha_s$  initiated signals such as the cAMP-PKA pathway. Using a “tool kit” of CHO-TSHR cells harboring CRE, NFAT, SRF or SRE response elements tagged to luciferase, as shown in Figure 1A, we identified potent and specific  $\text{G}\alpha_{q/11}$  selective small molecules. Our search found a molecule (MSq1) unlike our previously reported (17) agonist molecules which is biased toward  $\text{G}\alpha_{q/11}$ . TSH activates predominantly  $\text{G}\alpha_s$  (33) and  $\text{G}\alpha_{q/11}$  when used in high (non-physiologic) concentrations (34, 35). Coupling of  $\text{G}\alpha_{q/11}$  to the TSHR leads to activation of phospholipase C (PLC) which in turn triggers the release of intracellular calcium  $[\text{Ca}^{2+}]$ , and NFAT and alternatively activates protein kinase C (PKC) and its downstream effector

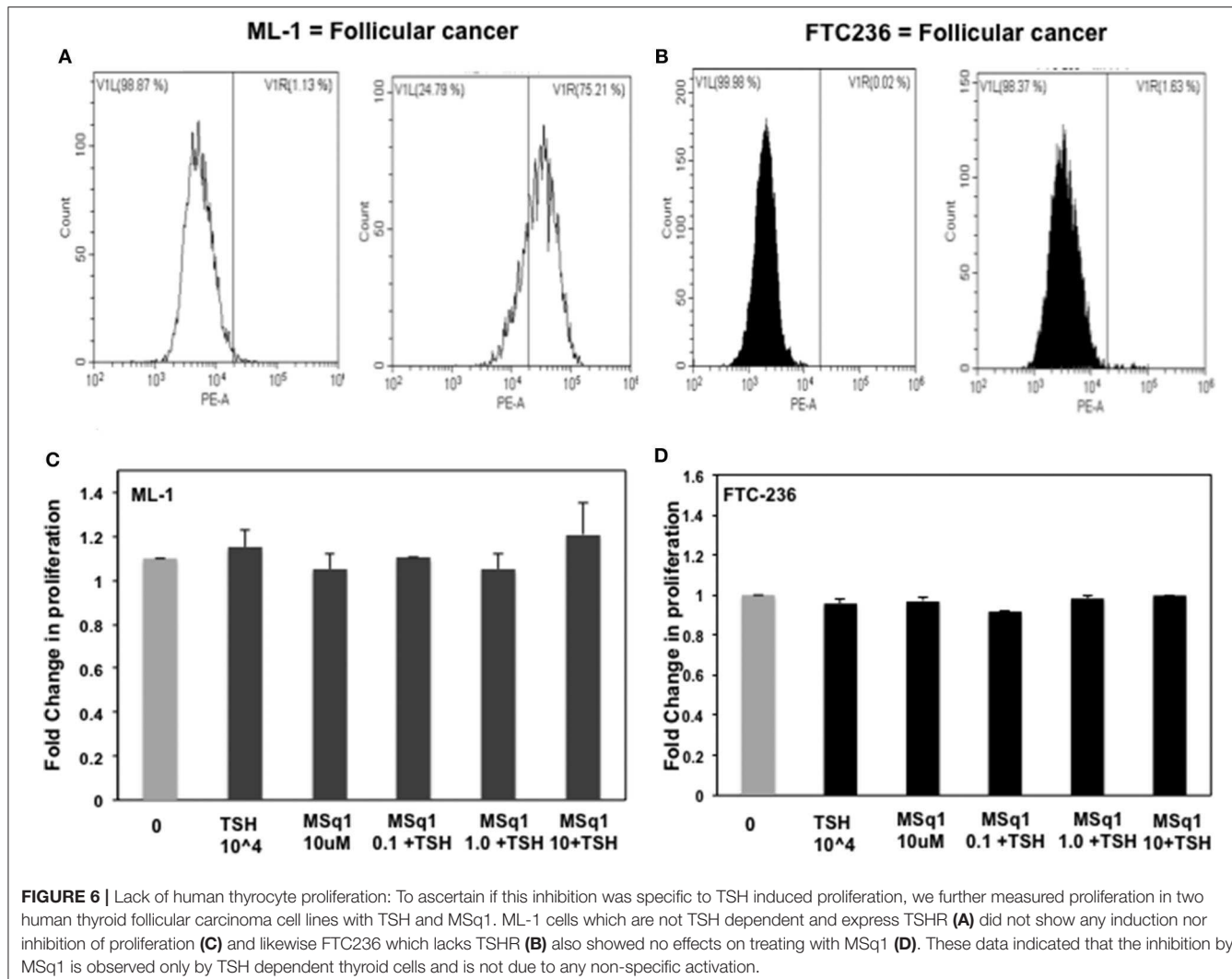


**FIGURE 6 |** Lack of human thyrocyte proliferation: To ascertain if this inhibition was specific to TSH induced proliferation, we further measured proliferation in two human thyroid follicular carcinoma cell lines with TSH and MSq1. ML-1 cells which are not TSH dependent and express TSHR **(A)** did not show any induction nor inhibition of proliferation **(C)** and likewise FTC236 which lacks TSHR **(B)** also showed no effects on treating with MSq1 **(D)**. These data indicated that the inhibition by MSq1 is observed only by TSH dependent thyroid cells and is not due to any non-specific activation.

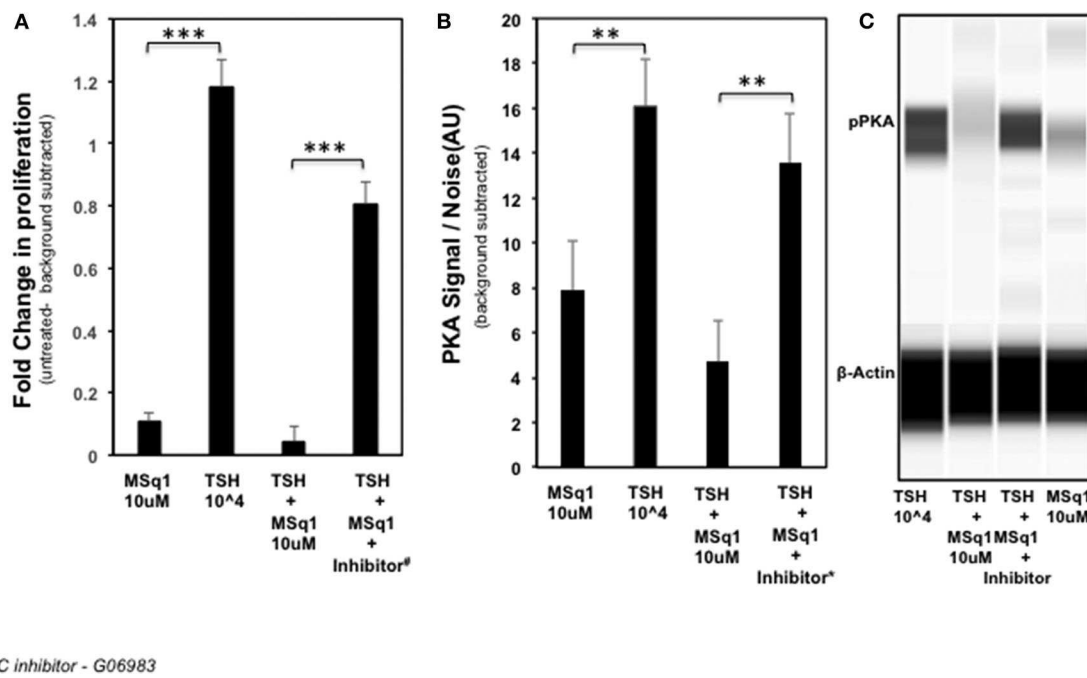
MAP kinase (MAPK). The normal physiological consequences of activating  $G\alpha_s$  in thyrocytes are proliferation, hormone synthesis and thyroglobulin (Tg) iodination (29, 36). However, the physiological or pathophysiological control of  $G\alpha_{q/11}$  signaling in thyrocytes or extrathyroidal TSHRs is not well-characterized despite multiple reports. For example, conditional deletion of  $G\alpha_{q/11}$  in mouse thyroid resulted in hypoplastic thyroid glands and severe hypothyroidism (34). It has also been shown that  $G\alpha_{q/11}$ -PKC dependent activation in TSHR transfected papillary cancer cells (line FTC236) resulted in the upregulation of a class of redox and metal ion scavengers which are cysteine-rich proteins known as metallothioneins (MTs) (37). Studies have also shown an indirect relationship of  $G\alpha_{q/11}$  activation to thyroid peroxidase formation (34, 38) and a congenital hypothyroidism phenotype (39).

Our docking studies with a modeled TMD (28) showed that the  $G\alpha_{q/11}$  activator molecule binds within the hydrophobic pocket of the TMD. By this analysis we saw that in addition to overlapping contacts with our agonist MS438 ( $G\alpha_s$  dominant), the MSq1 molecule also made contact with some unique residues helping to explain its selective allosteric  $G\alpha_{q/11}$  activation

(Table 1). Furthermore, docking MSq1 to the TSH binding surface of the ECD resulted in docking scores that were more than 4 kcal/mol weaker than the top scores observed when docked to the TMD. Such differences represent  $\sim$ 786 times weaker binding indicating that this molecule, like our previously reported small molecules, is can be a allosteric molecule (17).

Despite tremendous progress into the molecular mechanism concerning contacts and activation of G proteins by GPCRs (40, 41) our understanding as to how structurally distinct ligands may lead to the stabilization of different “active states” of the receptors remains open. Homology modeling of the TSHR with the  $G_q$  heterodimer combined with mutational analysis of the transmembrane domain has indicated the principal determinants leading to the complex interaction (4, 14, 42) suggesting spatial conformation for selective G protein activation.

In this study, we observed that MSq1 is an activator of PLC (Figure 4A) and its downstream effectors—PKC and NFAT activation (Figure 4B). MSq1 showed increased phosphorylation of PKC. However, we failed to see any up regulation in the



#PKC inhibitor - G06983

**FIGURE 7 |** Mechanistic studies on inhibition of thyrocyte proliferation. In order to examine if PKC activation by MSq1 was leading to inhibition of TSH induced proliferation we used a PKC inhibitor (G06983). **(A)** FRTL5 cells were stimulated by MSq1 alone, TSH 10<sup>4</sup> μM alone, TSH + MSq1 and TSH + MSq1 + PKC inhibitor for 48 h as indicated. MSq1 effectively inhibited TSH induced proliferation but in the presence of this PKC inhibitor (2 μM); proliferation was restored in these cells. Note that the untreated cell data were subtracted as background from all the data (\*\*P < 0.0001). **(B)** Since the possible mechanism of this inhibition was likely to be the result of PKA suppression by the induced PKC, we quantitated the levels of pPKA in the treated samples using immunoblotting in the Wes system. As observed here, PKA was significantly decreased with MSq1 as opposed to TSH alone. This suppression of PKA was released when the cells were treated with TSH and MSq1 in the presence of the PKC inhibitor. The untreated cell data were subtracted as background from all the data (\*\*P < 0.001). **(C)** The lane representations of the WES output are similar to the data that is represented in panel B and shown here with phosphor PKA and β actin bands.

mRNA levels of thyroid specific genes in contrast to the effect of TSH or our small molecule agonist MS438. On examining the proliferation of these cells, MSq1 alone did not induce any proliferation as seen with MS438 or TSH. It is generally accepted that the proliferation of thyroid cells by TSH is mediated in large part by the cAMP-PKA pathway (43, 44). In contrast, the MSq1 molecule showed the unique ability to suppress TSH induced proliferation. Since we did not observe any blockade of TSH induced cAMP by MSq1 (Figure S4) we hypothesized that suppression must be due to interference with the cAMP-PKA pathway and most likely by PKC activation. There exists cross-talk in downstream signaling of GPCRs (45) and it has been previously shown that PKC can suppress PKA induced activation (46) and functional interference between cAMP/PKA and PKC pathways is possible (47, 48). Thus, experiments carried out in the presence of a PKC inhibitor confirmed that inhibiting PKC in the presence of MSq1 and TSH showed a marked reduction in the suppressive effect of MSq1 on proliferation. Furthermore, pPKA levels showed a significant increase after exposure to the PKC inhibitor. The only study which supports a physiological role for the Gα<sub>q/11</sub> mediated signaling pathway in TSH induced hormone synthesis (34) was performed in Gα<sub>q/11</sub> knock out mice. However, the action of MSq1 on proliferation is opposite to the Gα<sub>q/11</sub> study. Our model would suggest that overt activation

of the cAMP-PKA pathway by high concentrations of TSH leading to increased proliferation might be kept in check by the PLC-PKC pathway via Gq and thus maintain a balance in the endogenous proliferative capacity of thyrocytes differing with data that contradicts much of the literature which suggested that TSH stimulates differentiation and not proliferation of normal human thyrocytes (49).

In conclusion, we have identified a novel Gα<sub>q/11</sub> biased modulator of the TSHR with inhibitory effects on thyrocyte proliferation. The data illustrate the intertwining molecular mechanisms leading to this action. This raises the prospect of modulating biased TSHR signaling for more specific pharmacologic responses.

## DATA AVAILABILITY STATEMENT

The raw data supporting the conclusions of this article will be made available by the authors, without undue reservation, to any qualified researcher.

## AUTHOR CONTRIBUTIONS

RL responsible for design, execution of the experiments, data analysis, and manuscript writing. SM helped in the experiments

1141 with western blots. RM helped in PCR experiments. BT helping  
 1142 in carrying out some facets experiments. MM did the modeling and  
 1143 *in-silico* docking studies. TD helped in data analysis and finalizing  
 1144 of the manuscript.

## 1145 1146 FUNDING

1148 This work was supported in part by National Institute of Health  
 1149 (NIH) grant DK069713, the Segal Family Endowment, and the  
 1150 Veterans Administration Merit Award Program (to TD).

## 1154 REFERENCES

1. Davies TF, Ando T, Lin RY, Tomer Y, Latif R. Thyrotropin receptor-associated diseases: from adenoma to Graves disease. *J Clin Invest.* (2005) 115:1972–83. doi: 10.1172/JCI26031
2. Laugwitz KL, Allgeier A, Offermanns S, Spicher K, van Sande J, Dumont JE, et al. The human thyrotropin receptor: a heptahelical receptor capable of stimulating members of all four G protein families. *Proc Natl Acad Sci USA.* (1996) 93:116–20. doi: 10.1073/pnas.93.1.116
3. Neumann S, Krause G, Claus M, Paschke R. Structural determinants for g protein activation and selectivity in the second intracellular loop of the thyrotropin receptor. *Endocrinology.* (2005) 146:477–85. doi: 10.1210/en.2004-1045
4. Kleinau G, Jaeschke H, Worth CL, Mueller S, Gonzalez J, Paschke R, et al. Principles and determinants of G-protein coupling by the rhodopsin-like thyrotropin receptor. *PLoS One.* (2010) 5:e9745. doi: 10.1371/journal.pone.0009745
5. Furmaniak J, Sanders J, Nunez Miguel R, Rees Smith B. Mechanisms of Action of TSHR Autoantibodies. *Horm Metab Res.* (2015) 47:735–52. doi: 10.1055/s-0035-1559648
6. Sanders J, Chirgadze DY, Sanders P, Baker S, Sullivan A, Bhardwaja A, et al. Crystal structure of the TSH receptor in complex with a thyroid-stimulating autoantibody. *Thyroid.* (2007) 17:395–410. doi: 10.1089/thy.2007.0034
7. Sanders P, Young S, Sanders J, Kabelis K, Baker S, Sullivan A, et al. Crystal structure of the TSH receptor (TSHR) bound to a blocking-type TSHR autoantibody. *J Mol Endocrinol.* (2011) 46:81–99. doi: 10.1530/JME-10-0127
8. Schaaerschmidt J, Huth S, Meier R, Paschke R, Jaeschke H. Influence of the hinge region and its adjacent domains on binding and signaling patterns of the thyrotropin and follitropin receptor. *PLoS One.* (2014) 9:e111570. doi: 10.1371/journal.pone.0111570
9. Schaaerschmidt J, Nagel MB, Huth S, Jaeschke H, Moretti R, Hintze V, et al. Rearrangement of the extracellular domain/Extracellular loop 1 interface is critical for thyrotropin receptor activation. *J Biol Chem.* (2016) 291:14095–108. doi: 10.1074/jbc.M115.709659
10. Marcinkowski P, Kreuchwig A, Mendieta S, Hoyer I, Witte F, Furkert J, et al. Thyrotropin receptor: allosteric modulators illuminate intramolecular signaling mechanisms at the interface of ecto- and transmembrane domain. *Mol Pharmacol.* (2019) 96:452–62. doi: 10.1124/mol.119.116947
11. Haas AK, Kleinau G, Hoyer I, Neumann S, Furkert J, Rutz C, et al. Mutations that silence constitutive signaling activity in the allosteric ligand-binding site of the thyrotropin receptor. *Cell Mol Life Sci.* (2011) 68:159–67. doi: 10.1007/s00018-010-0451-2
12. Wenzel-Seifert K, Seifert R. Molecular analysis of beta(2)-adrenoceptor coupling to G(s)-, G(i)-, and G(q)-proteins. *Mol Pharmacol.* (2000) 58:954–66. doi: 10.1124/mol.58.5.954
13. Moller S, Vilo J, Croning MD. Prediction of the coupling specificity of G protein coupled receptors to their G proteins. *Bioinformatics.* (2001) 17(Suppl. 1):S174–81. doi: 10.1093/bioinformatics/17.suppl\_1.S174
14. Kleinau G, Haas AK, Neumann S, Worth CL, Hoyer I, Furkert J, et al. Signaling-sensitive amino acids surround the allosteric ligand binding site of the thyrotropin receptor. *FASEB J.* (2010) 24:2347–54. doi: 10.1096/fj.09-149146
15. Neumann S, Padia U, Cullen MJ, Eliseeva E, Nir EA, Place RF, et al. An enantiomer of an oral small-molecule TSH receptor agonist exhibits improved pharmacologic properties. *Front Endocrinol (Lausanne).* (2016) 7:105. doi: 10.3389/fendo.2016.00105
16. Neumann S, Gershengorn MC. Small molecule TSHR agonists and antagonists. *Ann Endocrinol (Paris).* (2011) 72:74–6. doi: 10.1016/j.ando.2011.03.002
17. Latif R, Ali MR, Ma R, David M, Morshed SA, Ohlmeyer M, et al. New small molecule agonists to the thyrotropin receptor. *Thyroid.* (2015) 25:51–62. doi: 10.1089/thy.2014.0119
18. Neumann S, Eliseeva E, McCoy JG, Napolitano G, Giuliani C, Monaco F, et al. A new small-molecule antagonist inhibits Graves' disease antibody activation of the TSH receptor. *J Clin Endocrinol Metab.* (2011) 96:548–54. doi: 10.1210/jc.2010-1935
19. Marcinkowski P, Hoyer I, Specker E, Furkert J, Rutz C, Neuenschwander M, et al. A new highly thyrotropin receptor-selective small-molecule antagonist with potential for the treatment of graves' orbitopathy. *Thyroid.* (2019) 29:111–23. doi: 10.1089/thy.2018.0349
20. Latif R, Realubit RB, Karan C, Mezei M, Davies TF. TSH receptor signaling abrogation by a novel small molecule. *Front Endocrinol (Lausanne).* (2016) 7:130. doi: 10.3389/fendo.2016.00130
21. Luttrell LM, Maudsley S, Bohn LM. Fulfilling the promise of “Biased” G protein-coupled receptor agonism. *Mol Pharmacol.* (2015) 88:579–88. doi: 10.1124/mol.115.099630
22. Ulloa-Aguirre A, Reiter E, Crepieux P. FSH receptor signaling: complexity of interactions and signal diversity. *Endocrinology.* (2018) 159:3020–35. doi: 10.1210/en.2018-00452
23. White KL, Scpton AP, Rives ML, Bikbulatov RV, Polepally PR, Brown PJ, et al. Identification of novel functionally selective kappa-opioid receptor scaffolds. *Mol Pharmacol.* (2014) 85:83–90. doi: 10.1124/mol.113.089649
24. Tschammer N, Bollinger S, Kenakin T, Gmeiner P. Histidine 6.55 is a major determinant of ligand-biased signaling in dopamine D2L receptor. *Mol Pharmacol.* (2011) 79:575–85. doi: 10.1124/mol.110.068106
25. Morshed SA, Ma R, Latif R, Davies TF. How one TSH receptor antibody induces thyrocyte proliferation while another induces apoptosis. *J Autoimmun.* (2013) 47:17–24. doi: 10.1016/j.jaut.2013.07.009
26. Bradford MM. A rapid and sensitive method for the quantitation of microgram quantities of protein utilizing the principle of protein-dye binding. *Anal Biochem.* (1976) 72:248–54. doi: 10.1016/0003-2697(76)90527-3
27. Morshed SA, Latif R, Davies TF. Characterization of thyrotropin receptor antibody-induced signaling cascades. *Endocrinology.* (2009) 150:519–29. doi: 10.1210/en.2008-0878
28. Ali MR, Latif R, Davies TF, Mezei M. Monte Carlo loop refinement and virtual screening of the thyroid-stimulating hormone receptor transmembrane domain. *J Biomol Struct Dyn.* (2015) 33:1140–52. doi: 10.1080/07391102.2014.932310
29. Vassart G, Dumont JE. The thyrotropin receptor and the regulation of thyrocyte function and growth. *Endocr Rev.* (1992) 13:596–611. doi: 10.1210/er.13.3.596

## ACKNOWLEDGMENTS

We thank Dr. Bhasker Das from the Departments of Medicine and Pharmacological Sciences, Icahn School of Medicine at Mount Sinai for critical reading of our manuscript.

## SUPPLEMENTARY MATERIAL

The Supplementary Material for this article can be found online at: <https://www.frontiersin.org/articles/10.3389/fendo.2020.00372/full#supplementary-material>

1255 30. Davey RA, MacLean HE. Current and future approaches using genetically 1312 modified mice in endocrine research. *Am J Physiol Endocrinol Metab.* (2006) 1313 291:E429–38. doi: 10.1152/ajpendo.00124.2006

1256 31. Neumann S, Huang W, Titus S, Krause G, Kleinau G, Alberobello AT, 1314 et al. Small-molecule agonists for the thyrotropin receptor stimulate thyroid 1315 function in human thyrocytes and mice. *Proc Natl Acad Sci USA.* (2009) 1316 106:12471–6. doi: 10.1073/pnas.0904506106

1257 32. Neumann S, Pope A, Geras-Raaka E, Raaka BM, Bahn RS, Gershengorn MC. 1317 A drug-like antagonist inhibits thyrotropin receptor-mediated stimulation 1318 of cAMP production in Graves' orbital fibroblasts. *Thyroid.* (2012) 22:839– 1319 43. doi: 10.1089/thy.2011.0520

1258 33. Laurent E, Mockel J, van Sande J, Graff I, Dumont JE. Dual 1320 activation by thyrotropin of the phospholipase C and cyclic 1321 AMP cascades in human thyroid. *Mol Cell Endocrinol.* (1987) 1322 52:273–8. doi: 10.1016/0303-7207(87)90055-4

1259 34. Kero J, Ahmed K, Wettchureck N, Tunaru S, Wintermantel T, Greiner E, et al. 1323 Thyrocyte-specific Gq/G11 deficiency impairs thyroid function and prevents 1324 goiter development. *J Clin Invest.* (2007) 117:2399–407. doi: 10.1172/JCI 1325 30380

1260 35. Song Y, Massart C, Chico-Galdo V, Jin L, De Maertelaer V, Decoster 1326 C, et al. Species specific thyroid signal transduction: conserved 1327 physiology, divergent mechanisms. *Mol Cell Endocrinol.* (2010) 1328 319:56–62. doi: 10.1016/j.mce.2010.01.024

1261 36. De Felice M, Postiglione MP, Di Lauro R. Minireview: thyrotropin receptor 1329 signaling in development and differentiation of the thyroid gland: insights 1330 from mouse models and human diseases. *Endocrinology.* (2004) 145:4062– 1331 7. doi: 10.1210/en.2004-0501

1262 37. Back CM, Stohr S, Schafer EA, Biebermann H, Boekhoff I, Breit A, et al. 1332 TSH induces metallothionein 1 in thyrocytes via Gq/11- and PKC-dependent 1333 signaling. *J Mol Endocrinol.* (2013) 51:79–90. doi: 10.1530/JME-12-0200

1263 38. Song Y, Diessens N, Costa M, De Deken X, Detours V, Corvilain B, et al. Roles 1334 of hydrogen peroxide in thyroid physiology and disease. *J Clin Endocrinol 1335 Metab.* (2007) 92:3764–73. doi: 10.1210/jc.2007-0660

1264 39. Garcia M, Gonzalez de Buitrago J, Jimenez-Roses M, Pardo L, Hinkle PM, 1336 Moreno JC. Central hypothyroidism due to a TRHR mutation causing 1337 impaired ligand affinity and transactivation of Gq. *J Clin Endocrinol Metab.* 1338 (2017) 102:2433–42. doi: 10.1210/jc.2016-3977

1265 40. Mahoney JP, Sunahara RK. Mechanistic insights into GPCR-G 1339 protein interactions. *Curr Opin Struct Biol.* (2016) 41:247– 1340 54. doi: 10.1016/j.sbi.2016.11.005

1266 41. Rasmussen SG, DeVree BT, Zou Y, Kruse AC, Chung KY, Kobilka TS, et al. 1341 Crystal structure of the beta2 adrenergic receptor-Gs protein complex. *Nature.* 1342 (2011) 477:549–55. doi: 10.1038/nature10361

1267 42. Kleinau G, Neumann S, Gruters A, Krude H, Biebermann H. Novel insights 1343 on thyroid-stimulating hormone receptor signal transduction. *Endocr Rev.* 1344 (2013) 34:691–724. doi: 10.1210/er.2012-1072

1268 43. Jin S, Horneck FJ, Neylan D, Zakarija M, McKenzie JM. Evidence that 1345 adenosine 3',5'-monophosphate mediates stimulation of thyroid growth in 1346 FRTL5 cells. *Endocrinology.* (1986) 119:802–10. doi: 10.1210/endo-119-2-802

1269 44. Tramontano D, Moses AC, Veneziani BM, Ingbar SH. Adenosine 3',5'- 1347 monophosphate mediates both the mitogenic effect of thyrotropin and its 1348 ability to amplify the response to insulin-like growth factor I in FRTL5 cells. 1349 *Endocrinology.* (1988) 122:127–32. doi: 10.1210/endo-122-1-127

1270 45. Hur EM, Kim KT. G protein-coupled receptor signalling and cross- 1350 talk: achieving rapidity and specificity. *Cell Signal.* (2002) 14:397– 1351 405. doi: 10.1016/S0898-6568(01)00258-3

1271 46. Lesage GD, Marucci L, Alvaro D, Glaser SS, Benedetti A, Marzoni M, 1352 et al. Insulin inhibits secretin-induced ductal secretion by activation of 1353 PKC alpha and inhibition of PKA activity. *Hepatology.* (2002) 36:641– 1354 51. doi: 10.1053/jhep.2002.35537

1272 47. Laglia G, Zeiger MA, Leiprecht A, Caturegli P, Levine MA, Kohn LD, et al. 1355 Increased cyclic adenosine 3',5'-monophosphate inhibits G protein-coupled 1356 activation of phospholipase C in rat FRTL-5 thyroid cells. *Endocrinology.* 1357 (1996) 137:3170–6. doi: 10.1210/endo.137.8.8754735

1273 48. Sho KM, Okajima F, Abdul Majid M, Kondo Y. Reciprocal modulation 1358 of thyrotropin actions by P1-purinergic agonists in FRTL-5 thyroid cells. 1359 Inhibition of cAMP pathway and stimulation of phospholipase C-Ca2+ 1360 pathway. *J Biol Chem.* (1991) 266:12180–4.

1274 49. Morgan SJ, Neumann S, Marcus-Samuels B, Gershengorn MC. 1361 Thyrotropin stimulates differentiation not proliferation of normal 1362 human thyrocytes in culture. *Front Endocrinol (Lausanne).* (2016) 1363 7:168. doi: 10.3389/fendo.2016.00168

1275

1276

1277

1278

1279

1280

1281

1282

1283

1284

1285

1286

1287

1288

1289

1290

1291

1292

1293

1294

1295

1296

1297

1298

1299

1300

1301

1302

1303

1304

1305

1306

1307

1308

1309

1310

1311

1312

1313

1314

1315

1316

1317

1318

1319

1320

1321

1322

1323

1324

1325

1326

1327

1328

1329

1330

1331

1332

1333

1334

1335

1336

1337

1338

1339

1340

1341

1342

1343

1344

1345

1346

1347

1348

1349

1350

1351

1352

1353

1354

1355

1356

1357

1358

1359

1360

1361

1362

1363

1364

1365

1366

1367

1368